HOSTED BY

ELSEVIER

CrossMark

Available online at www.sciencedirect.com

ScienceDirect

Defence Technology 12 (2016) 272–276

www.elsevier.com/locate/dt

Experimental research on HEL and failure properties of alumina under impact loading

Xiao-wei FENG *, Jing-zhen CHANG, Yong-gang LU

Institute of Systems Engineering, China Academy of Engineering Physics, Mianyang 621900, China

Received 5 October 2015; revised 4 January 2016; accepted 20 January 2016

Available online 3 March 2016

Abstract

A series of plate impact experiments on alumina was conducted using a light gas gun in order to further investigate Hugoniot elastic limit (HEL) and failure properties of alumina under shock compression. The velocity interferometer system for any reflector (VISAR) was used to record the rear-free surface velocity histories of the alumina samples. According to the experimental results, the HELs of tested alumina samples with different thicknesses were measured, and the decay phenomenon of elastic wave in shocked alumina was studied. A phenomenological expression between HEL and thickness of sample was presented, and the causes of the decay phenomenon were discussed. The propagation of failure wave in shocked alumina was probed. The velocity and delayed time of failure wave propagation were obtained. The physical mechanism of the generation and propagation of failure was further discussed.

Keywords: Plate impact experiment; Alumina; Hugoniot elastic limit; Failure wave

1. Introduction

The interest to investigate the behavior of ceramics subjected to high velocity impact evolves mainly from their importance to manufacture the light-weight armor composites. The compressive strength and failure characteristics of ceramic armor under shock loading are the important factors for analyzing a ballistic performance against the penetrator. Understanding of the properties of the compressive strength and failure of ceramics under impact loading is essential in the design of improved impact resistant materials for dynamic structural and armor applications.

The Hugoniot elastic limit (HEL) is interpreted as the limit of elastic response and the onset of failure under dynamic uniaxial strain loading, which is used extensively in high velocity impact dynamics. During the past decades, the flyer plate impact test has been the most frequently reported experimental technique for measuring the HEL of material. The previous experimental results showed an interesting phenomenon of that the elastic precursor amplitude decreased with propagation distance in the alumina sample, which was termed as precursor decay [1–4]. However, Refs. [5,6] presented the conflicting results that no sign of such precursor decay was observed in tested alumina.

The failure wave, which is one of the most important discoveries in impact dynamics field over the last 20 years, is a new brittle failure mechanism of some brittle materials, such as glass and ceramics, etc., under compressive shock loading. It was observed by Rasorenov [7] and Kanel [8] through an observation of a small recompression signal on the free surface velocity history of shocked K19 glass. Continuing efforts have been made to confirm the existence of failure waves in other types of glasses [9–12] and ceramics, such as alumina [13,14], silicon carbide [15] and boron carbide [16]. The formation and propagation mechanisms of this failure phenomenon have been proposed over the last two decades. However, the understanding of the failure wave phenomenon is still far from complete because there are some disagreement and controversy between the available data and theoretical predictions. For example, up to now, it is not sure whether the propagating velocity of failure wave, which is a crucial parameter to characterize the failure wave phenomenon, is a constant or not under a certain dynamic loading. Refs. [7,8] reported that the failure wave velocity decreased with the increase in propagation distance in shock loaded materials. However, more researchers believed that the failure wave velocity in brittle materials is constant with the given external loading and increases with the increase in loading intensity. In this paper,

Peer review under responsibility of China Ordnance Society.

* Corresponding author. Tel.: +8608162493743.

E-mail address: xiaowei_feng@126.com (X.W. FENG).

http://dx.doi.org/10.1016/j.dt.2016.01.007

the velocity of failure wave in shocked alumina was measured by the VISAR technique. And the formation mechanism of failure wave of alumina was further analyzed.

2. Experiment

The density of the tested alumina, ρ0, is 3.896 g/cm^3, the measured longitudinal wave velocity cl is 9.259 km/s, the shear wave velocity cs is 5.557 km/s, and the Poisson ratio v is 0.218. The calculated sound velocity corresponding to the volume compressibility of the material is

$$cb = cl\sqrt{(1+v)/3(1-v)} = 6.671\ \mathrm{km/s}.$$

The composition of the tested alumina consists of 92.85% Al2O3, 4.89% SiO2, 0.36% CaO and 1.90% La2O3 by weight. We studied the samples in the form of disks with 40 mm in diameter and 4, 6, 8 and 10 mm in thickness. A 6 mm thick copper flyer was designed with the longitudinal wave velocity of 3490 m/s.

The double-thickness target developed in the study is shown in Fig. 1, in which two sub-targets are embedded into a two-hole target ring, with the impact surfaces of both the target ring and two sub-targets being rigorously set on one plane. The plate impact experiments under the one-dimensional strain condition were carried out on a Φ100 mm one-stage light gas gun, and two free surface velocity histories of each sub-target were recorded simultaneously by the VISAR technique. Impact velocities were measured to 1.5% accuracy using three pairs of electric signal pins and were all in the range of 439–445 m/s. So the samples were considered to undergo the same compressive state approximately.

3. Results and discussions

Fig. 2 shows the measured free surface velocity profiles of alumina samples with different thicknesses. These profiles show an initial elastic precursor wave followed by the onset of a dispersive inelastic wave which characterizes the material yielding. The onset point is denoted as HEL, which can be determined by the well-known relation

$$\sigma_{\mathrm{H}} = \frac{1}{2}\rho_0 c_{\mathrm{l}} u_{\mathrm{H}} \tag{1}$$

where ρ_0 is the density of alumina, c_{l} is the longitudinal wave velocity, and u_{H} is the free surface velocity.

However, the free surface velocity profiles of alumina show that the transition from elastic phase to inelastic phase occurs gradually. There is no sharp distinction between the elastic part and inelastic part. The rounded transition from the elastic part to inelastic part makes the unambiguous determination of HEL value difficult. We tried to distinguish a turning point of elastic phase to inelastic phase in Fig. 2, and obtained σ_{H} of alumina using Eq. (1), as shown in Table 1. It is noted that the HEL of alumina obtained in the present study ranges from 4.41 GPa to 5.59 GPa. These data and the HELs of other aluminas [4,17,18] similar in composition are presented in Fig. 3. It is shown that the HELs of tested alumina are lower than the data presented by others. The difference in the value of σ_{H} here may be attributed to the differences in the composition, density, preparation process of samples, or the distinction of turning point.

In order to investigate the properties of HEL of alumina under shocked loading, the HELs of tested alumina were plotted against the thicknesses of samples in Fig. 4. It is found that HEL of alumina decreases with the increase in sample thickness, which is termed as the elastic precursor decay. This phenomenon is considered to be similar to the phenomenon of size effect of other brittle materials, such as concrete and rock, namely the strength of brittle material decreases with the increase in its volume. However, the physical mechanism of this phenomenon is very complex and no complete satisfactory theory exists presently. A simpler model has been proposed to describe the size effect of brittle materials under compression

$$Y = A_0 + A_1 D^{-k} \tag{2}$$

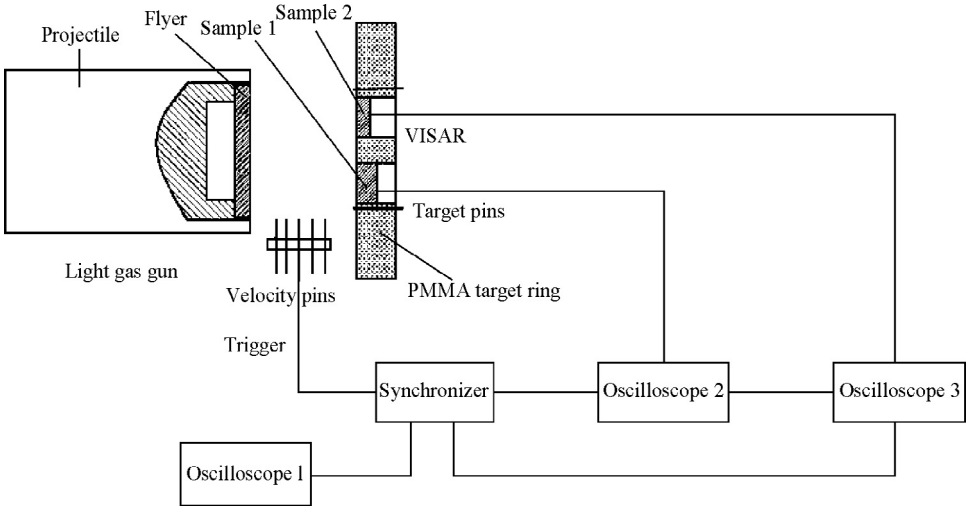

Fig. 1. Schematic diagram of double-target impact experimental setup.

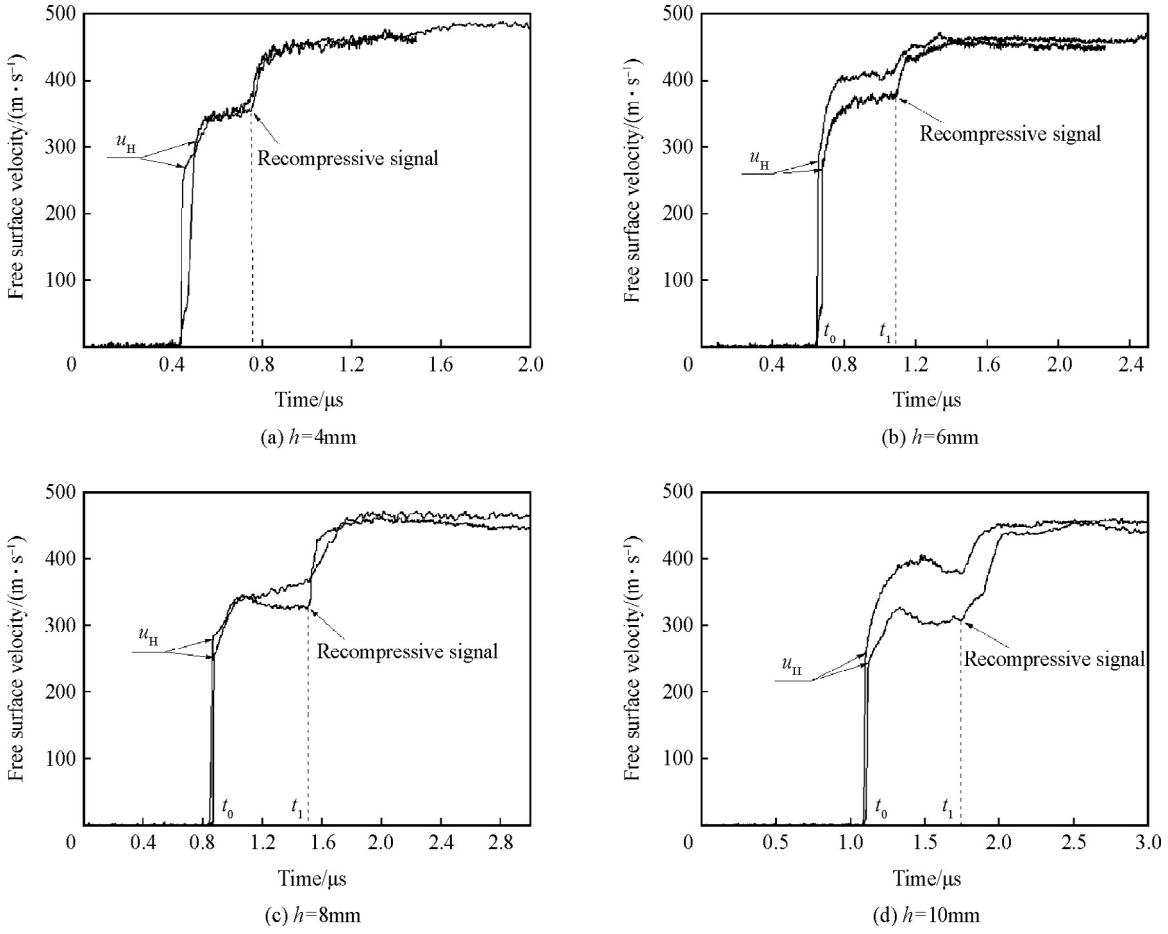

Fig. 2. Free surface velocity profiles of shocked alumina in present experiments.

where Y is the dynamic yield strength of material, D is the volume of sample, and A_0, A_1, and k are positive parameters. k is determined to be 0.4 for brittle materials [19]. In the present paper, Y is related to σ_H through the well-known relation

$$Y = \frac{1-2v}{1-v}\sigma_H \tag{3}$$

where D can be represented as $\pi r^2 h$. Because v and r are constants, Eq. (3) can be rewritten as

$$\sigma_{HEL} = A_0 + Bh^{-0.4} \tag{4}$$

A_0 and B can be determined to be 3.04 and 3.84, respectively, by fitting the experimental data shown in Fig. 4.

Table 1
Hugoniot elastic limits of alumina ceramics.

No.	Hsample/mm	u_H/(m·s^{-1})	σ_H/GPa
a	4	271.59	4.90
		309.74	5.59
b	6	277.43	5.00
		264.87	4.78
c	8	279.41	5.04
		251.17	4.53
d	10	257.36	4.64
		244.38	4.41

Murray et al. [4] studied this phenomenon in three grades of alumina through the stress–time measurements, and showed that the precursor decay effect was the greatest in the low purity aluminas. However, the further analysis [20] revealed that this phenomenon was probably a measurement artifact, resulting from the relatively slow response time of mangan in gauge. Obviously, the data obtained in our experiments did not support this point of view, which showed an apparent decay in HEL with the increase in sample thickness. VISAR is a non-contact

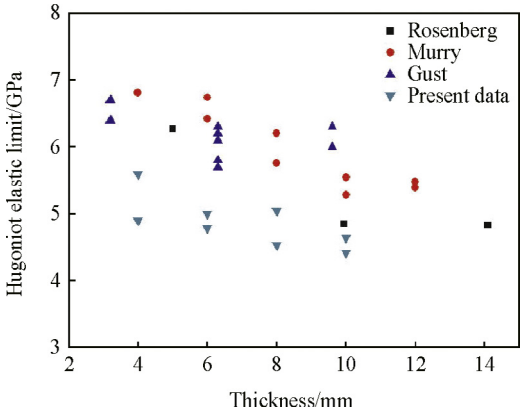

Fig. 3. HELs of aluminas under shock loading.

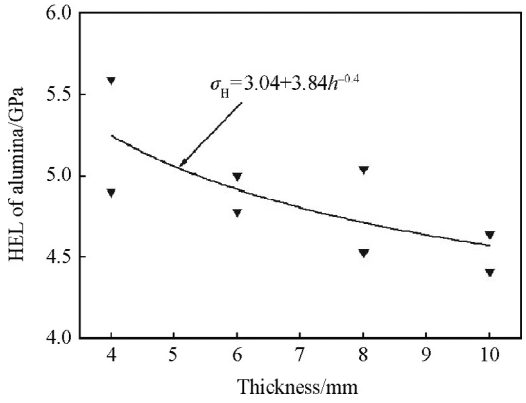

Fig. 4. HEL vs. thickness for tested alumina.

technique without measurement errors existing in stress measurement, so it can be deduced that this phenomenon is an essential characteristic of the alumina under shock loading. The HEL is known as a point of transition from elastic response to inelastic response, so the phenomenon of elastic precursor decay should be studied combined with the failure mechanism of shocked alumina. The previous works reported that cracking, dislocation activity and twinning were observed in shock-loaded alumina, even when the peak-shock stress is less than the magnitude of HEL [21–27]. In authors' opinion, the failure process occurring below HEL may play the dominant role in the phenomenon of elastic precursor decay. As is known to all, the evolution process of cracking or plasticity is an energy dissipation process essentially. In the region behind the elastic precursor wave, the preexisting microdetects act as stress concentrators and provide the nucleation sites for damage evolution, which dissipate the elastic energy. Thus, the longer distance the elastic wave passes through, the more elastic energy will be dissipated, which causes the amplitude of elastic wave decay.

From the free surface velocity profiles, we can also observe the apparent recompressive wave signals which are marked by dashed line in Fig. 5. This phenomenon is interpreted as a failure wave. It follows from consideration of the time–distance diagram shown in Fig. 5 that the failure waves meet the unloading waves reflected from the free surfaces of the samples with different thicknesses at the distance x_i and time t_i, as determined by Eq. (5)

$$t_{i0} = \frac{h_i}{c_l}$$
$$x_i = h_i - c_l \frac{t_{1i} - t_{0i}}{2}$$
$$t_i = \frac{t_{1i} + t_{0i}}{2} \tag{5}$$

Here, the longitudinal wave velocity c_l in the sample is assumed to be a constant during wave propagation. The arrival time t_{1i} of failure waves can be obtained from the free surface velocity profiles. The failure wave trajectories for the four samples with 4, 6, 8 and 10 mm in thickness are obtained by the Eq. (5) mentioned above as shown in Fig. 6. It can be seen from Fig. 6 that the four points locate just on a straight line in a good approximation, which can be fitted well by a linear equation between the time [t(μm)] and distance [x(mm)] as follows

$$t = 0.198x + 0.105 \tag{6}$$

From Eq. (6), it can also be seen that there exists an initial delay time for the failure wave on the impact surface, which is about 0.105 μs. This delay failure mechanism is considered to be related to the evolution of microdetects under impact loading, such as microcracks growth and accumulation, etc., which was discussed in our earlier works [13].

The propagating velocity of failure wave in test alumina can be also obtained from the trajectory, which is the slope of the trajectory curve about 5.051 km/s in Fig. 6. This velocity is apparently higher than those of the failure waves observed in the shocked glasses, where they are usually 1–3 km/s [7,10–12]. The formation mechanism of failure waves in shocked glasses is always interpreted as the activation and growth of microcracks on the impact surface [7,15]. From this point of view, the propagating velocity of failure wave should be slower than the limiting growth velocity of crack which is always slower than Rayleigh wave velocity [28]. Once the velocity of cracks reaches a limited value which is much slower than Rayleigh wave velocity, they tend to branch out [29]. The Rayleigh wave velocity in tested alumina can be calculated directly by the shear wave velocity and the Poisson's ratio as follows [28]

$$c_R = \frac{0.862 + 1.14v}{1 + v} c_s \approx 5.067 \text{ km/s} \tag{7}$$

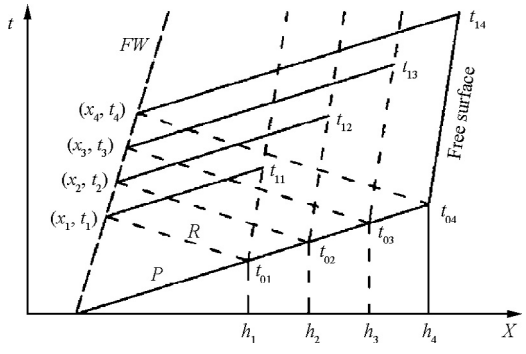

Fig. 5. The time–distance diagram for failure wave.

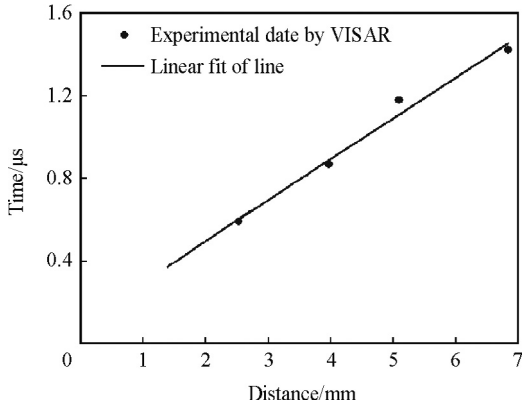

Fig. 6. Experimental data and its linear fitting line.

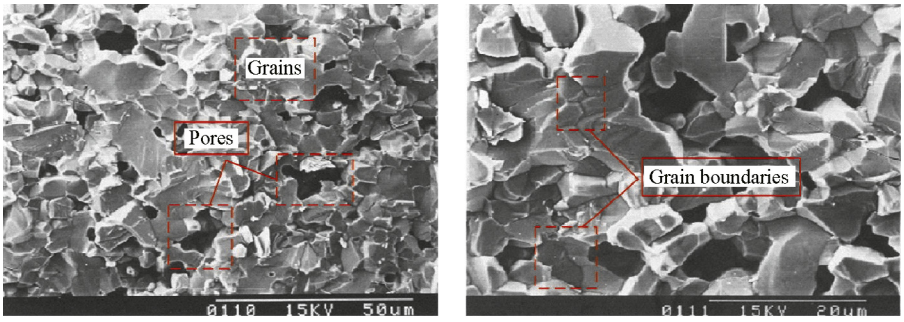

(a) (b)

Fig. 7. SEM micrographs of alumina samples.

It is shown that the failure wave velocity measured in tested alumina is very close to the Rayleigh wave velocity. Thus, the formation mechanism of failure waves in shocked alumina may be different from that in shocked glass.

According to the SEM micrographs of alumina sample shown in Fig. 7, it is known that the microstructure of alumina consists of alumina grains, pores and intergranular glassy phase. The grains and pores distribute randomly with the diameters of 1–15 μm. Intergranular glassy phase is distinct in a compact area. Pores and glassy phase weaken the mechanical capabilities of alumina, and these heterogeneous microstructures act as the stress concentrators. It has been well known that a high shear stress would be produced due to the large confining stress under the uniaxial strain loading. The localized stress concentrations are expected to arise from the propagation of cracks and flaws at grain boundaries. The failure is proposed to proceed essentially through rapid in situ grain boundary microcracks nucleation and comminution with very limited crack growth after a delay time once a shock wave travels through the sample. As the microcracks in situ nucleate in the stressed alumina and do not need time to transmit from the impact surface, the failure front with lower dynamic impedance in the shocked alumina could be detected much earlier from the rear surface, and it therefore gives a higher observed failure wave velocity. This failure mechanism is different from that in the shocked glass, but similar to that in the shocked rocks [30].

4. Summary

In this paper, the plate impact experiments were performed on aluminas with different thicknesses, and the free surface velocity histories of alumina samples were traced by VISAR technique. The HELs of tested alumina were obtained from the temporal curves of free surface velocity. We found an elastic precursor decay phenomenon in shocked alumina, and proposed that the physical mechanism of this phenomenon was related to the failure processes of shocked alumina occurring below HEL. Moreover, a simple model was applied to describe this phenomenon. In addition, the failure wave trajectory was derived from the free surface velocity histories, which presented the failure wave velocity of about 5.051 km/s under the given impact loading. The formation mechanism of failure waves in shocked alumina was proposed to proceed essentially through rapid in situ grain boundary microcracks nucleation, which was different from that in shocked glass.

Acknowledgments

The project is supported by the Science and Technology Development Foundation of China Academy of Engineering Physics (Grant No. 2014B0101009) and the National Natural Science Foundation of China (Grant No. 11502258, 11272300).

References

[1] Yaziv D, Yeshurun Y, Partom Y, Rosenberg Z. Shock compression of condensed matter-1987. APS Conference Proceedings; 1988. p. 297.
[2] Rosenberg Z, Brar NS, Bless SJ. J Phys Colloq 1988;49:707.
[3] Bourne NK, Rosenberg Z, Field JE, Crouch IG. J Phys IV 1994;4:269.
[4] Murray NH, Bourne NK, Rosenberg Z. J Appl Phys 1998;84:4866.
[5] Cagnoux J, Longy F. In: Schmidt SC, Holmes NC, editors. Shock waves in condensed matter 1987. Amsterdam: North-Holland; 1988. p. 293.
[6] Grady DE. Mech Mater 1998;29:181.
[7] Rasorenov SV, Kanel GI, Fortov VE, Abasehov M. High Press Res 1991;6.
[8] Kanel GI, Fortov VE, Rasorenov SV. Shock compression of condensed matter-1991. Elsevier Science Publishers BV; 1992. p. 451.
[9] Brar NS, Rosenberg Z, Bless SJ. J Phys IV 1991;1(C3):639.
[10] Bless SJ, Brar NS, Kanel GI, Rosenberg Z. J Am Ceram Soc 1992;75:1002.
[11] Bourne NK, Rosenberg Z, Field JE. J Appl Phys 1995;78:3736.
[12] Zhang YG, Duan ZP, Zhang LS, Ou ZC, Huang FL. Exp Mech 2011;51:247.
[13] Feng XW, Liu ZF, Chen G, Yao GW. Adv Appl Ceram 2012;110:335.
[14] Bourne NK, Millett JCF, Rosenberg Z, Murray N. J Mech Phys Solids 1998;46:1887.
[15] Bourne NK, Millett JCF, Pickup I. J Appl Phys 1997;81:6019.
[16] Bourne NK, Gray GT. Shock compression of condensed matter-2001. USA; 2001. p. 775.
[17] Rosenberg Z, Brar NS, Bless SJ. J Phys 1988;c3:707.
[18] Gust WH, Royce EB. J Appl Phys 1971;42:1.
[19] Bazant ZP, Xiang Y. J Eng Mech-ASCE 1997;123:162.
[20] Marom H, Sherman D, Rosenberg Z. J Appl Phys 2000;88:10.
[21] Chen MW, McCauley JW, Dandekar DP, Bourne NK. Nat Mater 2006;5:614.
[22] Longy F, Cagnoux J. J Am Ceram Soc 1989;72:971.
[23] Nemat-Nasser S. Ceram Trans 2002;134:403.
[24] Espinosa HD, Raiser G, Clifton RJ, Ortiz M. J Appl Phys 1992;72:3451.
[25] Merala TB, Chan HW, Howitt DG, Kelsey PV, Korth GE, Williamson RL, et al. Mater Sci Eng A Struct Mater 1988;105–106:293.
[26] Lankford J, Predebon WW, Staehler JM, Subhash G, Pletka BJ, Anderson CE. Mech Mater 1998;29:205.
[27] Rajendran AM, Dandekar DP. Int J Impact Eng 1995;17:649.
[28] Achenbach JD. Wave propagation in elastic solids. New York: North-Holland Publishing Company; 1973.
[29] Meyers MA. Dynamic behavior of materials. New York: John Wiley & Sons, Inc.; 1994.
[30] Chen D, He H, Jing F. J Appl Phys 2007;102:033519.